



BROADBAND NOISE MODELLING AND PREDICTION FOR AXIAL FANS

Michele DE GENNARO, Helmut KUEHNELT

*AIT Austrian Institute of Technology, Mobility Department
Giefinggasse 2, 1210 Vienna, Austria*

SUMMARY

In the frame of ventilation noise prediction and control the simulation of axial fan noise is still a challenge due to the high complexity of the aerodynamic phenomena involved. The objective of this paper is to provide a simplified technique for axial fan noise simulation based on a double approach: 2D BET or 3D CFD flow solution coupled with the BPM model for aeroacoustic model with 1/3 octave band and directivity noise predictions. Numerical noise predictions have been validated with experimental data available from literature achieving good results. Methodologies, limitations and potentialities of the approaches are discussed in order to shape a tool to be used for applied design and optimization of ventilation systems.

INTRODUCTION

Low noise design of HVAC (Heating, Ventilation and Air Conditioning) components receives today increasing attention in the frame of automotive, railway and aerospace industry in order to improve the comfort experienced by passengers. Despite the great progress in Computational Fluid Dynamics (CFD) the assessment of a reliable procedure for the numerical simulation of fan noise is still a challenge. In spite of the increasing popularity of very CPU-demanding approaches such as Detached Eddies Simulation (DES) and Large Eddies Simulation (LES) in the scientific community the adoption of such approaches does not guarantee reliable results. This is mainly due to the high complexity of the physical phenomena involved in aeroacoustic noise generation (e.g. turbulence and transition, instabilities, noise sources identification). Moreover for a large number of the problems the involved scales require very fine computational meshes, transient simulations and very small time step size, often resulting in prohibitive computational cost for 3D complex configurations. In general the strong demand of simplified models for industrial design and product optimization processes is not only restricted to axial fans ([5], [6], [18], [20], [21]) but can be regarded as a general topic aimed to achieve a deeper comprehension of the airborne noise phenomenon in ventilation, propulsion ([9], [23], [24]) and wind energy generation ([2], [3], [7], [8], [10], [19]).

The target of this paper is providing a fast, reliable and computationally inexpensive technique for broadband fan noise prediction based on the integration of an aerodynamic model for turbomachinery with the semi-empirical aeroacoustic model for aerofoil geometries of Brooks, Pope and Marcolini (BPM) published by NASA in 1989 [1]. According to the BPM model the noise generation mechanisms occurring on an aerofoil surface can be classified in three main categories: Turbulent Boundary Layer – Trailing Edge noise (TBL-TE), Laminar Boundary Layer – Vortex Shedding (LBL-VS) noise and Separation Stall (S-S) noise. TBL-TE is related to boundary layer turbulent eddies, LBL-VS to boundary layer laminar instabilities and the S-S to large scale vorticity that can be experienced at high Angle of Attacks. The mutual importance of these effects can be detected by evaluating the boundary layer integral quantities at the trailing edge location of the aerofoil: boundary layer thickness (δ) and displacement thickness (δ^*). The BPM model allows estimating the sound pressure level density spectrum in one-third octave band for a generic aerofoil as function of these quantities via an algebraic procedure based on the correlation of experimental data. This approach has been implemented and tested in an in-house tool for axial fan noise simulation. The test-case chosen for this study is based on geometrical and experimental data given by Carolus et al. [5], [6]. It is a 6 bladed axial fan with a diameter of 299 mm and an operative rotational speed of 3000 rpm providing a nominal volumetric flow rate of 0.59 m³/sec. The aerodynamic simulation of this fan has been performed with two approaches:

- Blade Element Theory (BET) coupled with XFOIL [15]
- CFD steady RANS (ANSYS-Fluent [16]) with Multiple Reference Frame (MRF) formulation to simulate the rotation

The noise spectra computed with the BPM model show a good agreement compared to the experimental data proving that the BPM model is able to capture sound pressure levels and broadband components over a wide range of frequencies (from 0.1 to 5 kHz), both coupled with BET/XFOIL as well as with CFD. Directivity effects were also taken into account. Additionally the interface to the BPM model is designed for automatic processing of data coming from the aerodynamic solvers mentioned above.

The acoustic modelling is a major topic for industrial fans in order to be applied in the frame of design, prediction and optimization of ventilation systems.

NUMERICAL FLOW MODELLING OF AXIAL FANS

Conceptually an axial fan can be defined as a rotating fluid machine whose practical objective consists in generating a difference of pressure between an upstream and a downstream region of the flow domain in order to transport a specific mass or volume rate of fluid (air). The aerodynamic behavior of such a machine can be assumed to be very similar to propeller and wind turbine aerodynamics and can be modeled by means of simplified approaches.

In this section a short overview of the BET is provided with a focus on the application to fans while in a second stage a brief review of the CFD approaches to turbomachinery is given. Later on, both approaches will be applied for the aerodynamic simulation of the test-case fan geometry and will be coupled with the semi-empirical BPM aeroacoustic model.

Blade Element Theory

BET is an analysis method that may be applied to propellers, fans, wind turbines and helicopter rotors dealing with a detailed description of flow conditions and loading of the blade. Conceptually BET is very similar to the strip theory for fixed wing aerodynamics assuming the blade composed by numerous strips of width dr . The aerodynamic behavior of each strip is determined by two factors: the geometry and the operating condition of the blade, which affect the asymptotic and rotational velocity components on the strip, and by upwash and downwash aerodynamic effects, which

determine a non-negligible correction of these components. The BET provides a very precise estimation of the real aerodynamic conditions (velocity and Angle of Attack, AoA) experienced on each blade strip while the forces (lift and drag) can be estimated using the 2D airfoil characteristics of the section. The global performance of the blade (e.g. thrust and torque for a propeller or flow rate for a fan) can be then evaluated integrating the local strip performances over the blade span.

Let us consider the Figure 1 where a blade moving with an axial velocity V and a rotational velocity ω is sketched. Moreover let us focus on the rotational velocity component experienced by the generic strip element located at a distance r from the axis, equal to ωr . Here the geometric wind velocity V_R , the effective wind velocity V_e , the axial and tangential induced velocity components w_a and w_t and the induced AoA α_i are reported. As it clearly appears from the sketch the real aerodynamic conditions experienced by the strip have to be determined estimating w_a and w_t to correct V and ωr . Then the effective AoA (calculated by subtracting the quantity $\varphi + \alpha_i$ from the sectional design angle β) and the effective velocity V_e can be computed to estimate the sectional lift and drag forces (dL and dD) by means of 2D aerodynamic characteristics of the airfoil.

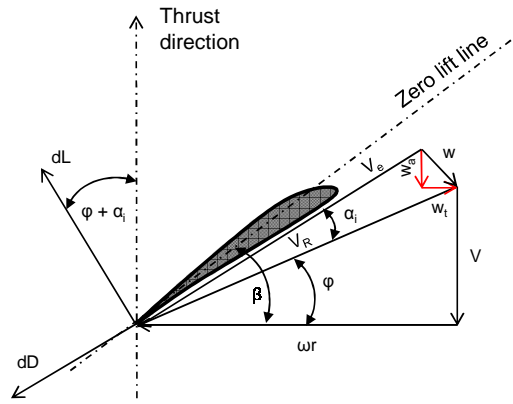


Figure 1: Blade element strip sketch.

According to [12] the BET can be formulated with 2 different approaches. The first approach assumes as unknown the induced AoA α_i and suggests the explicit algebraic equation (1) where σ is the blade solidity (defined as $N \cdot b / \pi \cdot r$), N the number of blades, b the sectional chord length, $C_{l\alpha}$ the sectional lift coefficient gradient ($\sim 2\pi$) and F the Prandtl correction factor (2). Once α_i is computed the w_a and w_t components can be estimated by geometrical considerations (2) and the effective AoA and velocity can be computed to calculate the sectional loads.

$$\alpha_i = \frac{1}{2} \left[- \left(\operatorname{tg} \varphi + \frac{\sigma C_{l\alpha}}{8F \cos \varphi} \right) + \sqrt{\left(\operatorname{tg} \varphi + \frac{\sigma C_{l\alpha}}{8F \cos \varphi} \right)^2 + \frac{\sigma C_{l\alpha}}{2F \cos \varphi} (\beta - \varphi)} \right] \quad (1)$$

$$F = \frac{2}{\pi} \cos^{-1} \left[e^{\frac{(r-1)N}{2 \sin \varphi}} \right] \quad w_a = V_R \alpha_i \cos(\varphi + \alpha_i) \quad w_t = V_R \alpha_i \sin(\varphi + \alpha_i) \quad (2)$$

The second approach assumes as unknown the induced tangential velocity w_t and suggests the implicit algebraic equation (3) where w_a is given by (4). Then α_i can be easily estimated (4) and therefore the effective AoA and velocity computed.

$$w_t = \frac{\omega \sigma V_e C_{l\alpha}}{8rF} \left[\beta - \tan^{-1} \left(\frac{w_t}{w_a} \right) \right] \sqrt{\left(r - \frac{w_t}{\omega R} \right)^2 + \frac{1}{4} \left[\sqrt{\left(\frac{V}{\omega R} \right)^2 + 4 \frac{w_t}{\omega R} \left(r - \frac{w_t}{\omega R} \right) + \left(\frac{V}{\omega R} \right)^2} \right]^2} \quad (3)$$

$$w_a = \frac{1}{2} \left[\sqrt{V^2 + 4w_t(\omega r - w_t)} - V \right] \quad \alpha_i = \tan^{-1} \left(\frac{w_t}{w_a} \right) - \varphi \quad (4)$$

It is important to highlight that during the passages leading to equation (1) a linearization hypothesis has been assumed. This assumption consists in considering the induced AoA α_i small compared to φ and consequently w_a and w_t small compared to V_R . As this is usually true for propellers, where the two approaches provide nearly the same results, it could be not valid for fans, where the induced component is often only the axial component (since the translational velocity is zero). Therefore we recommend using the implicit nonlinear approach for fan simulation. For further details about the BET we refer to classical literature [12], [13] and [14].

The BET has been implemented into an in-house fan simulation tool and interfaced with the 2D boundary element aerodynamic solver XFOIL [15] for the bi-dimensional strip simulation and coupled with the BPM aeroacoustic model. Further details about the BET/BPM integration will be provided later.

CFD Modelling for Turbomachinery

In general CFD deals with numerical simulation of fluid-related phenomena via the solution of the Navier-Stokes (N-S) fluid equations. It is a set of 5 scalar elliptic partial differential equations for the balance of mass, momentum and energy in a fluid domain. The direct numerical resolution of these equations is hardly performed since the strong non-linearity and the spatial and temporal resolution required to properly describe the turbulent scales results in such immense computational cost that it is never affordable for complex 3D industrial geometries. Therefore the solution of the N-S equations is usually approached by means of two techniques: the averaging of the equations (leading to the Reynolds-Averaged N-S, RANS) and the filtering of the equations (leading to the Large Eddy Simulation, LES). In short the RANS technique averages the equations over a sufficiently long time period in order to eliminate the turbulent fluctuations but to keep the time dependence of the averaged quantities. This averaging process introduces the problem of mathematical closure of the averaged equations which results in the introduction of a turbulence model. On the other hand the LES technique filters the equations using the computational grid size as limit for either directly resolving the turbulent scales of large eddies or modeling the subgrid scales in a RANS-like manner with a subgrid turbulence model. Since the grid resolution is directly linked to the results resolution, the LES has to be performed with highly accurate computational grids making this approach usually much more computationally demanding than the RANS but in general also more accurate. Sometimes hybrid approaches such as Detached Eddy Simulation (DES) or Zonal LES can be used to preserve the high accuracy of the LES with a lower computational cost.

In the frame of turbomachinery problems the effect of the rotation is introduced by means of two different techniques: the Sliding Mesh approach (SLM), where the entire computational grid is moved, and the Multiple Reference Frame (MRF), where the rotation is considered by transforming the equations in a moving reference frame. Usually the SLM approach is considered more computationally expensive since it requires a transient simulation and grid handling capabilities, while the MRF is less computationally demanding and allows performing the steady simulation. The second approach can be already enough accurate in a number of practical applications.

Choosing the right approach in every CFD modelling situation is often subordinated to a trade-off between the level of detail of the solution required and the computational load that can be afforded. In most of the cases concerning aeroacoustic simulation the effects of the turbulent scales cannot be neglected imposing the adoption of the LES with a consequent huge computational load. In this framework the adoption of CPU-saving approaches is a key-issue, especially for the integration of the aeroacoustic simulation into optimization cycles.

For our analysis we decided to use the steady RANS-MRF approach to simulate the aerodynamic performances of the fan and then we coupled the RANS solution with the BPM method. This choice was made because the BPM requires as input only the integral boundary layer quantities at the blade trailing edge which can be easily estimated with a steady RANS calculation. Moreover the possibility

to keep the computational load as low as possible was also one of the main targets of our work, in order to make it possible for industrial design problems. The simulations were performed with the commercial software ANSYS-Fluent [16]. Further details about computational setup, CAD model and computational grid will be provided later.

NUMERICAL (SEMI-EMPIRICAL) MODELLING OF AIRBORNE NOISE

As already mentioned in the introduction of this paper the noise generated by an aerodynamic surface can be classified in general into 3 main categories: Turbulent Boundary Layer - Trailing Edge noise (TBL-TE), Laminar Boundary Layer - Vortex Shedding (LBL-VS) noise and Separation Stall (S-S) noise. The TBL-TE mechanism (Figure 2, left-A) arises when a large region of turbulent boundary layer appears on the surface and is related to the turbulent eddies noise production providing typically a broadband noise spectrum. On the other hand the LBL-VS mechanism (Figure 2, left-B) arises when laminar instability conditions appear on the aerodynamic surface establishing a laminar bubbles fluctuation mechanism able to provide a very sharp and peaked noise spectrum [4]. Finally when large separation regions appear, large eddy structures are generated (e.g. Von Karman vortices) and the S-S mechanisms (Figure 2, left-C) arises, providing a broadband noise spectrum peaked nearby the main frequency of the vortices.

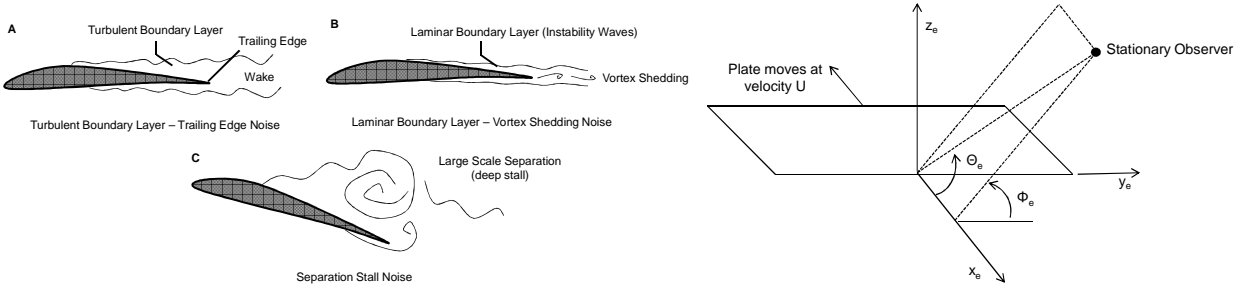


Figure 2: Noise generation mechanisms classification according to [1]. Turbulent B.L. - Trailing Edge (left-A). Laminar B.L. - Vortex Shedding (left-B) - Separation-Stall (left-C). Noise directivity angles (right).

This classification was given by Brooks et al. [1] as result of an extensive research campaign targeted to achieve a deep physical comprehension of the airfoil self generated noise phenomena as well as to provide simplified numerical models for reliable noise predictions in aeronautic applications.

$$\left\{ \begin{array}{l}
 SPL_{TBL-TE-P} = 10 \log \left(\frac{\delta_p^* M^5 L D_h}{r_e^2} \right) + A \left(\frac{St_p}{St_1} \right) + (K_1 - 3) + \Delta K_1 \\
 SPL_{TBL-TE-S} = 10 \log \left(\frac{\delta_s^* M^5 L D_h}{r_e^2} \right) + A \left(\frac{St_s}{St_1} \right) + (K_1 - 3) \\
 SPL_{S-S} = 10 \log \left(\frac{\delta_s^* M^5 L D_h}{r_e^2} \right) + B \left(\frac{St_s}{St_2} \right) + K_2 \\
 SPL_{LBL-VS} = 10 \log \left(\frac{\delta_p^* M^5 L D_h}{r_e^2} \right) + G_1 \left(\frac{St'}{St'_{peak}} \right) + G_2 \left(\frac{R_c}{R_{c,o}} \right) + G_3 (\alpha^*)
 \end{array} \right. \quad (5)$$

$$SPL_{TOT} = 10 \log \left(10^{\frac{SPL_{TBL-TE-P}}{10}} + 10^{\frac{SPL_{TBL-TE-S}}{10}} + 10^{\frac{SPL_{S-S}}{10}} + 10^{\frac{SPL_{LBL-VS}}{10}} \right) \quad (6)$$

Moreover they also mentioned additional noise generation mechanisms which can appear in particular cases (e.g. bluntness noise, wing-tip noise, asymptotic turbulence noise), which are neglected in our approach. It is based on a set of 4 algebraic equations (5) to predict TBL-TE

pressure side contribution, TBL-TE suction side contribution, S-S contribution and LBL-VS contribution, respectively. The total SPL is computed according to (6).

In equations (5) the δ and δ^* are the boundary layer thickness and the displacement thickness calculated at the trailing edge of the aerofoil, M is the Mach number, L is the span length, r_e the distance between the trailing edge and the receiver location, and A , B , $K_{1,2}$, ΔK_l and $G_{1,2,3}$ empirical functions based on a set of Strouhal numbers (St), Reynolds number (R_c) and AoA (α^*). These empirical functions have been implemented as given in [1] and [19]. Moreover p and s subscripts refer to pressure and suction side, respectively.

Directivity effects due to the longitudinal (Θ_e) and the transversal (Φ_e) visual angles (Figure 2 – right) of the receiver with respect to the noise source and to the Mach number of the flow past the trailing edge (M_c) are taken into account by means of the correction coefficient D_h (7). Please note that the directivity coefficient D_h only applies if the TBL-TE model produces a high frequency noise (up to a threshold AoA condition calculated by the model). For higher AoA nearly fully stalled conditions are experienced and the turbulent noise components are neglected ($SPL_{TBL-TE-P} = SPL_{TBL-TE-S} = -\infty$) while the S-S component remains and it is characterized by a low-frequency spectrum. This new component is given in (8), where A' is a low-frequency semi-empirical function and D_l the low-frequency directivity factor.

$$D_h = \frac{2 \sin(1/2\Theta_e) \sin^2 \Phi_e}{(1 + M \cos \Theta_e) [1 + (M - M_c) \cos \Theta_e]^2} \quad (7)$$

$$SPL_{S-S} = 10 \log \left(\frac{\delta_s^* M^5 L D_l}{r_e^2} \right) + A' \left(\frac{St_s}{St_2} \right) + K_2 \quad D_l = \frac{\sin^2 \Theta_e \sin^2 \Phi_e}{(1 + M \cos \Theta_e)^4} \quad (8)$$

The BPM model as provided by NASA has been implemented and tested in our tool and validated with the NASA provided experimental data for 4 different noise generation conditions involving major contributions of all noise models described above. Moreover it has been applied for noise prediction of the DU96 aerofoil for wind turbines applications [2]. The results reported in that paper show a good agreement between experimental and computational noise spectra for 8 different conditions tested, highlighting the great potentialities offered by this approach in the frame of airborne noise prediction.

TEST-CASE GEOMETRY AND WORK-FLOW

The test-case geometry and the experimental data used as reference in this paper originate from the work of Carolus et al. [5]. It is a 6-bladed axial fan with a diameter of 299 mm operated at a nominal rotational speed n of 3000 rpm corresponding to a tip Mach number of 0.14. The blade profile is the NACA 4509 with a design angle ranging from 48 deg at the root to 17.8 deg at the tip while the blade chord goes from 71.9 mm at the root to 56.7 mm at the tip (Figure 3). The blade is mounted on a cylindrical-shaped hub with a semi-spherical head with a diameter of 135 mm. The Reynolds number experienced on the blade varies from 90 k at the root to about 190 k at the tip. The fan is designed to provide a volumetric flow rate of 0.59 m³/sec operated in nominal conditions and it was tested in duct housing, instrumented with turbulence control devices, boundary layer removal devices and anechoic tube termination. Since the fan has been simulated in free air condition, the effect of the duct on the noise spectra was neglected, keeping in mind that it could lead to a discrepancy in the level between experimental and computational data. Further details concerning the effect of the duct will be provided later.

A pair of microphones was located on a circle with a radius of one meter around the center of the fan. The first receiver was located on the rotational axis (M1) while the second was located at an angle of 45 deg to the rotational axis (M2). For details concerning the aerodynamic standards used for tests,

microphones type, accuracy and tolerance of the results and test chamber type please refer to [5] and [6].

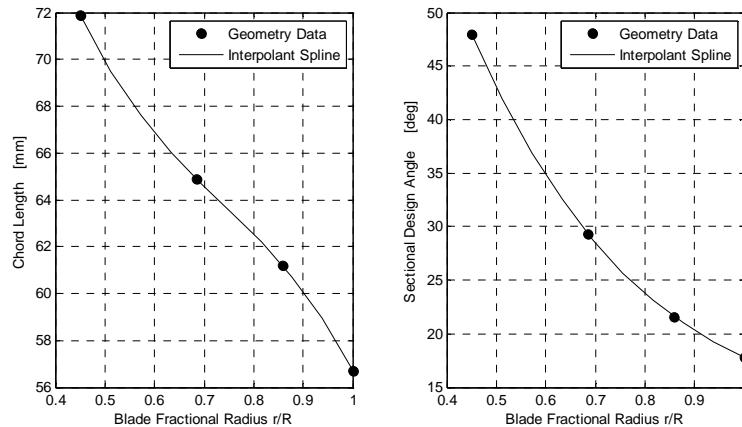


Figure 3: Axial fan blade geometry data. Chord length vs aerofoil radial position (left).
 Design angle vs aerofoil radial position (right).

In order to build up the blade geometry the chord length and the sectional design angle over the span dimension have been computed as spline of the 4 numerical values provided in [5] (Figure 3) and a CAD model of the blade consisting of 10 aerofoil sections was built.

A blade CAD module was implemented in an in-house analysis tool developed in MATLAB whose structure is provided in Figure 4. The 2D BEM software XFOIL is used as preprocessor to generate the aerofoil geometry that is imported by the CAD module to generate the blade. In the first branch of the diagram of Figure 4 (left side) the blade aerodynamic analysis and the boundary layer integral quantities analysis are performed by the BET module and boundary layer module. Both steps require the interface to XFOIL to estimate 2D aerofoil forces characteristics and the boundary layer integral quantities. Optionally the BET can use XFOIL in viscid or inviscid mode.

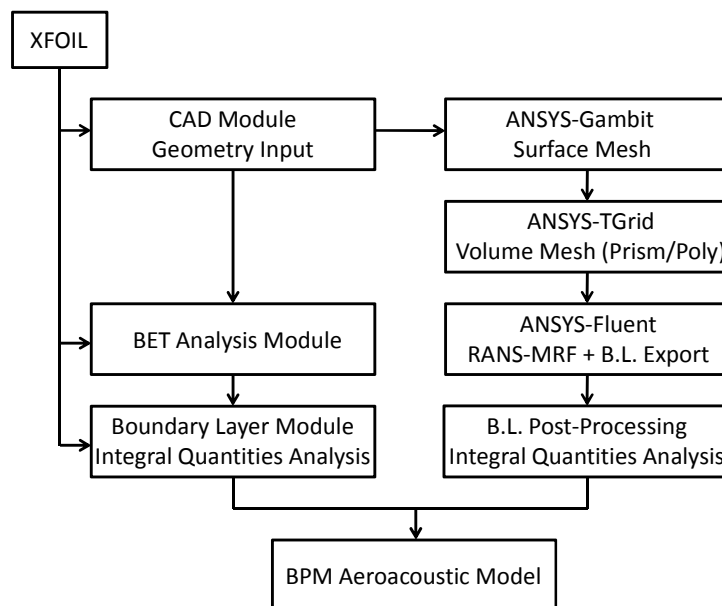


Figure 4: Axial fan noise simulation workflow

For the second branch (right side) the CAD module exports the geometry to ANSYS-Gambit where the blade is mounted on the hub and the surface mesh is generated. The surface mesh is then handed over to ANSYS-TGrid where a hybrid volume mesh is generated consisting of 20 layers of prism

cells extruded over the blade surface and polyhedral cells filling the rest of the computational domain.

The boundary layer prisms region of the grid is designed to provide a sufficient number of cells in the physical boundary layer (never less than 15) and a suitable value of y^+ (~ 1) on the blade surface for the operating condition considered. The mesh cells number achieved is 2.4M per blade. The aerodynamic simulation is then performed with ANSYS-Fluent using a steady RANS-MRF approach with periodic boundary conditions on the side walls (only 1 blade simulated) and $k-\omega$ SST turbulence model. The boundary layer profiles at the trailing edge of the blade are extracted by means of a series of rakes which are then post-processed to evaluate the integral quantities δ and δ^* . A picture of the CAD model and the details of the computational grid are provided in Figure 5.

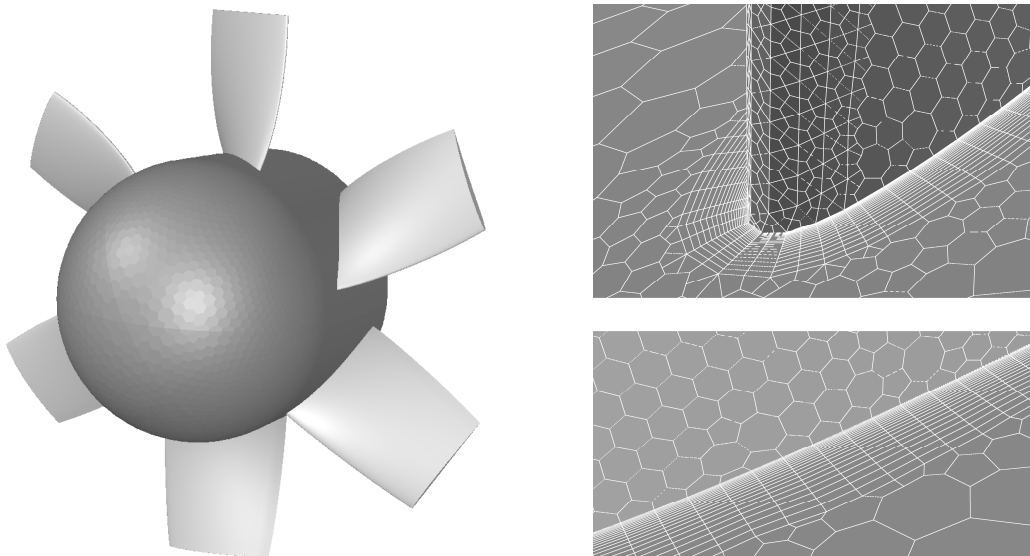


Figure 5: Axial fan CAD model (left). Details of the hybrid prism/polyhedral computational grid, blade leading edge (right-top), blade surface and boundary layer prisms extrusion (right-bottom).

The aeroacoustic simulation is then performed using the boundary layer parameters coming either from the BET/XFOIL analysis or from the CFD analysis for 10 span locations. The total SPL is then estimated with a logarithmic sum of the SPL referred to each blade slice. The left branch of the tool chain outlined in Figure 4 is a “fast simulation track” providing results with very low computational cost (CPU time of minutes) involving only simplified models (BET/BPM) plus the 2D BEM model (XFOIL). The second branch (right side in Figure 4) is a “slow simulation track” which involves the entire 3D CFD simulation process. It is important to highlight that all the passages of the slow simulation track (CAD modelling, mesh generation, simulation and post-processing) are automatized resulting in a quite low overall computational cost for the whole CFD-based simulation process.

RESULTS AND CONCLUSIONS

This last paragraph of the paper is dedicated to the description and discussion of results achieved with the BET/BPM and CFD/BPM procedures. In both cases the fan operates in open air while it is assumed ducted in the experimental setup, leading to discrepancies that have to be minimized via a correlation procedure. A critical discussion of these discrepancies and the advantage and disadvantages of the approaches adopted are given in order to understand limitations and potentialities of the suggested techniques.

BET/BPM Results

A first aerodynamic analysis of the fan previously described was performed with the BET techniques determining aerofoil characteristics by XFOIL viscid calculations. The aerodynamic solution achieved with the BET is given in Figure 6 - left, where the effective blade sectional angle ($\alpha_e = \beta - \varphi - \alpha_i$ with reference to Figure 1), the effective velocity (V_e) and the axial induced velocity component (w_a) are reported. The α_e quantity gives useful information about the aerodynamic conditions experienced by the blade over the span direction as well as about the noise sources that can be expected in the root/tip region of the blade. In this operational condition the root of the blade works mostly in separated and pre-stalled conditions (AoA ~ 10 -15 deg, $Re \sim 10^5$) with a consequent predominance of the S-S model in this region, while the tip of the blade works mostly in attached condition and we should expect a predominance of the TBL-TE-P/S models arising from this region. This has been also proved imposing a lower α_e as input to the BPM model showing a significant reduction of the contribution of the S-S model. Moreover V_e gives an estimation of the real velocity conditions and an estimation of the noise source relative magnitude, while w_a allows to estimate the volumetric flow rate integrating the axial induced velocity over the frontal circular surface of the fan. The nominal flow rate computed with BET is $0.605 \text{ m}^3/\text{sec}$, deviating $+2.5\%$ from the experimental value.

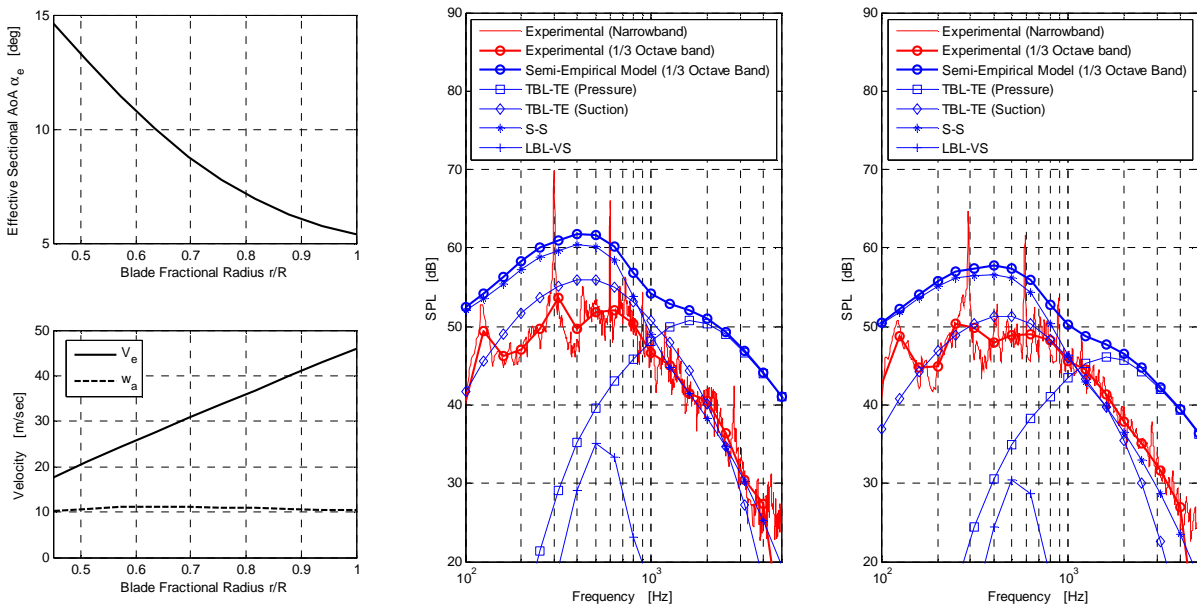


Figure 6: BET results, effective sectional AoA (left-top), effective velocity and axial induced velocity (left-bottom). BET/BPM noise spectra computed for the microphone M1 (center) and M2 (right).

Then a boundary layer analysis based on XFOIL was performed. Natural transition hypothesis (e^N method with $N = 9$) was imposed for all blade strips and the displacement thickness was evaluated with the integral boundary layer approach provided by the solver [25], [26] and [27]. It is important to highlight that XFOIL predictions are in principle not fully reliable in the low Reynolds number regimes (less than 0.5 M as in this case) since the solver is not able to properly handle laminar separation bubbles or large scale separations. Nevertheless we decided to apply it straightforward in our in-house tool. Additionally the boundary layer thickness was estimated by scaling the displacement thickness of a factor of 4 for the pressure and 2 for the suction side.

Acoustic results computed with the BPM model are given in Figure 6 - center and right. Narrowband and one-third octave band experimental spectra (red lines) [11] are compared with the SPL contributions coming from the above mentioned noise models (blue lines) for frequencies ranging from 0.1 to 5 kHz. No corrections were applied to match computed levels to experiments. From a first analysis it seems clear that for both microphones the numerical prediction overestimates the SPL

of about 10 dB over the whole frequency range considered. This overestimation can be related to the inaccuracies coming from the XFOIL predictions in the low Reynolds number conditions experienced in this case. In fact XFOIL shows the tendency to over-predict aerodynamic performance retarding the stall and this is also confirmed by a local strip lift coefficient analysis. Moreover it is important to highlight that there could be a possible mitigation effect on the experimental data due to the presence of the duct. Furthermore the predominant noise contribution comes from the S-S model (noise peak at approximately 0.4 kHz) while the TBL-TE suction and pressure models contribute to the mid and high frequency levels (over 0.8 kHz). The superposition of these models gives rise of a bump in the spectrum located approximately at 0.9 kHz that can be seen also in experimental data. Relative levels between the two microphone locations considered are quite well predicted thanks to the directivity model. No major contributions arise from the LBL-VS model.

CFD/BPM Results

As second step of our analysis the CFD simulation of the test-case fan was performed with a steady RANS-MRF approach. In this case the volumetric flow rate was estimated integrating the flux of the velocity field over a circular surface located immediately above the blade, achieving a stationary value of $0.57 \text{ m}^3/\text{sec}$, deviating -3% from the experimental value. Boundary layer data was extracted at 8 different span locations, from the 20% to the 90% of the blade span extension (r/R ranges from 0.51 to 0.94) with a constant step size of 10%. The root and the tip strip locations were excluded as the boundary layer profiles are considered to be too distorted by 3D effects. Both suction and pressure side boundary profiles were extracted at the trailing edge storing the velocity magnitude and the total pressure. The final profiles for the 80% rake ($r/R = 0.88$) are provided in Figure 7 - left. The upper cut-off of the boundary layer was assumed to be placed on the border of the viscid part of the flow field in which the total pressure changes. It has been located where the slope of a linear regression of a sliding window containing 4 different consequent values of the total pressure profile exhibits an angular deviation to the local vertical direction less than 5 deg. The predicted cut-off is reported by the blue squares on the y-axis in Figure 7 - left. This cut-off procedure has been chosen since it showed satisfying robustness and accuracy performances for different geometries and mesh types.

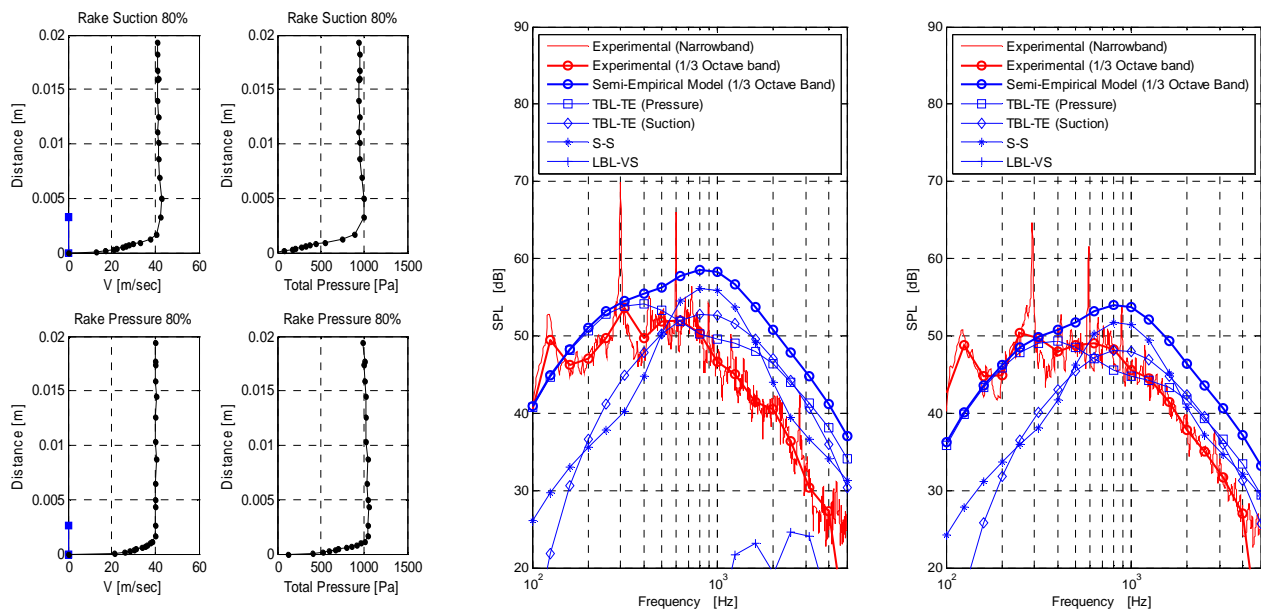


Figure 7: CFD boundary layer velocity magnitude and total pressure profiles for a rake located at the 80% of the blade span, suction surface (left-top) and pressure surface (left-bottom). CFD/BPM noise spectra computed for the microphone M1 (center) and M2 (right).

With the boundary layer upper limit δ , the boundary layer displacement thickness δ^* was computed according to [2], [17]. Acoustic predictions for the CFD/BPM model are again compared with experimental data given in Figure 7 - center and left. The CFD/BPM predictions show a general overestimation of the spectrum by 10 dB compared to experiments that is rather constant from 0.8 to 5 kHz. Also in this case no corrections have been applied to the data. Comparing BET/BPM and CFD/BPM predictions the latter approach seems to better predict the spectral slope from the frequency of the maximum SPL to higher frequencies, but somehow underestimates the level in the low frequency range (from 0.1 to 0.5 kHz). We interpreted the better agreement of this model in the high frequency range as result of the more reliable aerodynamic simulation achieved by the RANS model. Compared to the XFOIL results the RANS model describes better the viscous effects for the Reynolds number range involved. It should be kept in mind that the experimental data was obtained for a loaded fan (with the duct and the turbulence generator) giving large tonal components while the computations deal with an unloaded case where the broadband noise is the prominent source. This explains the low frequency range disagreement and the missing of the Blade Passing Frequency (BPF) peaks. In this case the level arising from the S-S model is less predominant. The balance between the pressure and suction TBL-TE models results to be different compared to the BET/BPM case. The contribution of the LBL-VS model is again negligible and the relative levels between the two microphones are well predicted.

CONCLUSIONS

In conclusion both BET/BPM and CFD/BPM approaches have been applied to simulate SPL spectrum of an axial fan. Predicted noise spectra show to be in agreement with experimental data with a tendency to overestimate the sound pressure level. The overestimation is predominant for the BET/BPM predictions due to the XFOIL's results for separated regions over the blade; therefore the CFD/BPM approach allows achieving better results. Furthermore the authors suggest correlating the data to use the proposed approaches for industrial purposes. The computational effort of both approaches is quite low making them suitable to be embedded into design and optimization loops.

ACKNOWLEDGEMENTS

The authors are grateful to the EC for the support to the present work performed within the EU FP7 Marie Curie ITN project VECOM (Grant Agreement 213543).

BIBLIOGRAPHY

- [1] T. F. Brooks, D. S. Pope, M. A. Marcolini – *Airfoil Self-Noise and Prediction*, NASA Reference Publication 1218, **1989**
- [2] M. De Gennaro, H. Kuehnelt – *Semi-Empirical Modelling of Broadband Noise for Aerofoils*, AIP Conference Proceedings Journal, Vol. 1389, pp. 1498-1502, **2011**
- [3] M. De Gennaro – *Computational Fluid Dynamics and Computational Aeroacoustics for Turbomachinery with emphasis on High Speed Propellers and Vertical Axis Wind Turbines*, Ph.D. Thesis in Industrial Engineering, University of Naples Federico II (Italy), **2010**
- [4] M. De Gennaro, A. Hueppe, H. Kuehnelt, M. Kaltenbacher – *Numerical Prediction of Laminar Instability Noise for NACA 0012 Aerofoil*, AIP Conference Proceedings Journal, Vol. 1389, pp. 78-81, **2011**
- [5] T. Carolus, M. Schneider, H. Reese – *Axial flow fan broad-band noise and prediction*, Journal of Sound and Vibration, 300, 50-70, **2007**

- [6] H. Reese, T. Carolus, C. Kato – *Numerical Prediction of the Aeroacoustic Sound Sources in a Low Pressure Axial Fan with Inflow Distortion*, Proceedings of Fan Noise Conference, **2007**
- [7] S. Oerlemans, P. Migliore – *Aeroacoustic Wind Tunnel Tests of Wind Turbine Airfoils*, AIAA Paper 2004-3042, **2004**
- [8] S. Oerlemans – *Wind Tunnel Aeroacoustic Tests of Six Airfoils for Use on Small Wind Turbines*, National Aerospace Laboratory NLR, NREL/SR-500-35339, **2004**
- [9] M. Herr – *Design Criteria for Low Noise Trailing Edges*, AIAA Paper 2007-3470, **2007**
- [10] W. Devenport, R. A. Burdisso, H. Camargo, E. Crede, M. Remillieux, M. Rasnick, P. Van Seeters – *Aeroacoustic Testing of Wind Turbine Airfoils*, Subcontract Report NREL/SR-500-43471, **2010**
- [11] D. A. Bies, C. H. Hansen – *Engineering Noise Control* 4th Edition, Taylor & Francis Spon Press, **2009**
- [12] H. Glauert – *Airplane Propellers*, in *Aerodynamic Theory*, Ed. W.F. Durand, Vol. IV, pp. 169-360, Berlin Julius Springer, **1935**
- [13] H. Glauert – *The Element of Airfoil and Airscrew Theory*, Cambridge Science Classics, **1947**
- [14] B. W. McCormick – *Aerodynamics of V/STOL Flight*, Academic Press, **1967**
- [15] M. Drela – *XFOIL 6.9 User-Guide*, Massachusetts Institute of Technology, **2001**
- [16] ANSYS Inc. – *ANSYS-Fluent Theory Guide*, **2010**
- [17] H. Schlichting *Boundary Layer Theory* McGraw Hill, **1979**
- [18] T. Carolus, M. Schneider – *Review of Noise Prediction Methods for Axial Flow Fans*, Internoise Conference Proceedings, **2000**
- [19] P. Fuglsang, H. A. Madsen – *Implementation and Verification of an Aeroacoustic Noise Prediction Model for Wind Turbines*, Risø-R-867(EN), **1996**
- [20] T. Carolus, M. Stremel, M. Schneider – *Tragflügelerschall: Anwendung der Messungen von Brooks, Pope und Marcolini auf Ventilatorlärm*, DAGA Proceedings, **2000**
- [21] S. Moreau, M. Henner, D. Casalino, J. Gullbrand, G. Iaccarino, M. Wang – *Toward the Prediction of Low-Speed Fan Noise*, Center for Turbulence Research, Proceedings of the Summer Program, **2006**
- [22] M. Roger, S. Moreau, M. Wang – *An Analytical Model for Predicting Airfoil Self-Noise using Wall-Pressure Statistics*, Center for Turbulence Research, Annual Research Briefs, **2002**
- [23] M. De Gennaro, D. Caridi, M. Pourkashanian – *Ffowcws Williams-Hawkings Acoustic Analogy for Simulation of NASA SR2 Propeller Noise in Transonic Condition*, ECCOMAS CFD 2010 Conference Proceedings, ID 1364 pp.1-16, ISBN: 978-989-96778-1-4, **2010**
- [24] M. De Gennaro, D. Caridi, C. de Nicola – *Noise Prediction of NASA SR2 Propeller in Transonic Condition*, AIP Conference Proceedings Journal, ISBN: 978-0-7354-0831-9, Vol. 1281, pp. 167-170, **2010**
- [25] R. Eppler – *Turbulent Airfoils for General Aviation*, Journal of Aircraft, Vol. 15, No. 2, **1978**
- [26] T. Cebeci – *An Engineering Approach to the Calculation of Aerodynamic Flows*, Springer ISBN 3-540-66181-6, **1999**
- [27] M. Drela, M. B. Giles – *Viscous-Inviscid Analysis of Transonic and Low Reynolds Number Airfoils*, AIAA-86-1786-CP, **1986**